

Recent Developments of NEMO: Detection of EUV Wave Characteristics

**O. Podladchikova, A. Vuets, P. Leontiev
& R. A. M. Van der Linden**

Solar Physics

A Journal for Solar and Solar-Stellar
Research and the Study of Solar
Terrestrial Physics

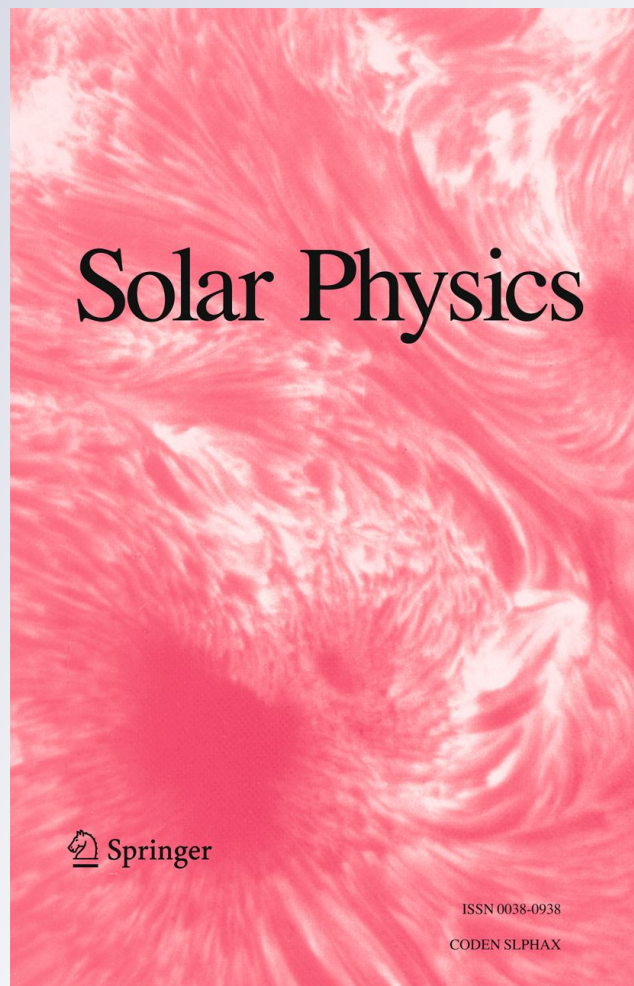
ISSN 0038-0938

Volume 276

Combined 1-2

Sol Phys (2012) 276:479-490

DOI 10.1007/s11207-011-9894-3



Your article is protected by copyright and all rights are held exclusively by Springer Science+Business Media B.V.. This e-offprint is for personal use only and shall not be self-archived in electronic repositories. If you wish to self-archive your work, please use the accepted author's version for posting to your own website or your institution's repository. You may further deposit the accepted author's version on a funder's repository at a funder's request, provided it is not made publicly available until 12 months after publication.

Recent Developments of NEMO: Detection of EUV Wave Characteristics

O. Podladchikova · A. Vuets · P. Leontiev ·
R.A.M. Van der Linden

Received: 16 March 2011 / Accepted: 1 November 2011 / Published online: 29 November 2011
© Springer Science+Business Media B.V. 2011

Abstract Recent developments in space instrumentation for solar observations and increased telemetry have necessitated the creation of advanced pattern recognition tools for different classes of solar events. The Extreme Ultraviolet Imaging Telescope (EIT) onboard the SOHO spacecraft has uncovered a new class of eruptive events on the solar disk, which are often identified as signatures of the initiation of coronal mass ejections (CMEs). The development of an automatic detection tool of these signatures is an important task. The Novel EIT Wave Machine Observing (NEMO) code (<http://sidc.be/nemo>) is an operational tool that automatically detects EUV waves using a sequence of EUV images. NEMO applies techniques based on the general statistical properties of the underlying physical mechanisms of eruptive events. Originally, the technique was applied to images taken with the EIT telescope. In this work, the most recent updates of the NEMO code are presented. These updates include calculations of the area of the dimming region, a novel clustering technique for the extraction of dimming regions, and new criteria to identify eruptive dimmings based on their complex characteristics. The efficiency of NEMO has been significantly increased and now permits the extraction of dimming regions observed near the solar limb and also the detection of small-scale events. Furthermore, the catalogs of solar eruptive events based on the updated NEMO may include a larger number of physical parameters associated with the dimming regions.

Keywords Corona · Coronal mass ejections · Flares · Instrumentation and data management · Low coronal signatures

O. Podladchikova (✉) · A. Vuets · P. Leontiev · R.A.M. Van der Linden
The Solar-Terrestrial Centre of Excellence, Royal Observatory of Belgium, Ringlaan-3, 1180 Brussels,
Belgium
e-mail: Elena.Podladchikova@stce.be

O. Podladchikova
Institute of Applied System Analysis, National Polytechnic University of Ukraine, Pobeda 37,
03056 Kiev, Ukraine

1. Introduction

A sudden energy release in the solar corona is a source of powerful electromagnetic disturbances in the near-terrestrial environment. Solar flares and coronal mass ejections (CMEs) can trigger geomagnetic storms that may affect terrestrial communications and the reliability of power systems. The most hazardous space weather events are associated with CMEs (Gopalswamy, 2004; Gosling *et al.*, 1990; Kahler, 1992; Richardson, Cliver, and Cane, 2001; Zhukov, 2004). Thus, CMEs and flares are our principal objects of detection and cataloging. However, their automatic detection is not simple, due to their complex characteristics. A number of methods to detect flares and CMEs in different wavelengths with different instrumental limitations have been reviewed by Robbrecht and Berghmans (2005). Today, a large number of instruments accessible to the space community monitor solar flares and CME events on a regular basis. Several data sources are available for consultation in real or near-real time in the case of solar flares.

The Solar Flare Automatic Detector in the Solar Soft package, which is based on recognition of bursts in the total X-ray flux from GOES-2, provides a solar flare catalog that is automatically constructed and is available on the website (http://www.lmsal.com/solarsoft/latest_events). A full catalog of solar flares observed by different instruments is manually constructed by the NOAA Space Weather Center in Boulder, Colorado, USA. The information is provided to the community with a one-day delay (<http://www.swpc.noaa.gov/ftppdir/indices/events>). The detection of CMEs has traditionally been based on the manual recognition of features moving radially outwards from the Sun using coronagraph data. The full CME catalog based on SOHO/LASCO observations is manually constructed by N. Gopalswamy's group (http://cdaw.gsfc.nasa.gov/CME_list). Significant progress was recently achieved in the automatic detection and cataloging of CMEs by the CACTUS software using SOHO/LASCO and STEREO/SECCHI data (<http://sidc.be/cactus>) (Robbrecht and Berghmans, 2004). This has led to near real-time alerts (a six-hour delay) being issued to the space weather community.

The growing interest in space weather effects has increased the accuracy level required in CME detection and forecast. In situ measurements are unable to address the problem of the prediction of solar eruptive events that can be extremely hazardous to space-based technological systems. However, solar surface observations may provide such information in advance and increase the forecast time of CME prediction. Furthermore, the increasing processing power of computers and the evolution in image processing and pattern recognition techniques have made possible the development of automatic detection tools for the solar drivers of space weather events.

During the last decade, the extreme ultraviolet (EUV) solar imaging from space has revealed a rich diversity of solar disk events, such as global waves, eruptive dimmings, and so-called "EUV wave" phenomenon (Thompson *et al.*, 1998). The EUV Imaging Telescope (EIT) onboard SOHO (Delaboudinière *et al.*, 1995) has provided high cadence EUV images of the solar corona continuously from early 1997 until 1 August 2010. The EUV waves are usually triggered by solar flares or sudden disappearance of filaments and appear as global bright features propagating in the solar corona followed by intensity dimness (dimming) as seen in EUV.

The first catalog of large-scale EUV waves was manually constructed by Thompson and Myers (2009) and accounted for the years 1997–1998. In contrast to the detection of solar flares and CMEs, which is based on the recognition of distinctive signatures (intensity bursts or global structures propagating in the plane of the sky), the detection of EUV waves is not easy. These waves are characterized by their low intensity variations with respect to the

level of general background and present a large variety in morphology and can last for tens of minutes.

The EUV waves are among the best indicators of large-scale reorganization of coronal magnetic fields (Plunkett *et al.*, 1998; Biesecker *et al.*, 2002; Harra and Sterling, 2001). Their appearance precedes the visibility of CMEs in coronagraphs and they thus provide one of the first signatures of CMEs. The EUV observations of these signatures precede the detection of the CME in a coronagraph field of view by a few hours and can be processed much faster than coronagraphic images (*i.e.* less images are required for detection). Consequently, real-time observations of eruptive dimmings ending with the EUV wave phenomenon might improve the issuing times of CME alerts.

The first proof-of-principle demonstration for the automated detection of EUV waves was based on the statistical properties of the eruptive EUV on-disk events and was proposed by Podladchikova and Berghmans (2005). The physical properties of the on-disk precursors of CMEs drastically modify higher-order statistical properties of the image sequences. Based on this proof-of-principle demonstration, an algorithm was developed to detect EUV waves and eruptive dimmings. The algorithm was tested with the calibrated SOHO/EIT data of the 1997–1998 period and successfully extracted the events listed in the EUV wave catalog of Thompson and Myers (2009). In 2006, the Novel EUV Wave Machine Observing (NEMO) (<http://sidc.be/nemo>) operational tool was developed in order to automatically detect EUV waves using real-time quick-look EIT images and to extract eruptive dimming events. NEMO was based on a series of high level image processing techniques suitable for extracting eruptive features from the EUV solar disk images under complex solar conditions. One particularly important feature of NEMO is its capability to detect among a large family of solar dimmings those that are always present on the EUV solar disk and those that are connected to CMEs.

The operation of NEMO allowed the automatic construction of a catalog with eruptive dimmings and EUV waves detected in the image sequences of SOHO for the period 1997–2010. The majority of the events listed in the catalog were identified as signatures of CME initiation (using CME catalogs). In contrast to the detection methods based on coronagraph data, NEMO could also detect even the initiation of faint halo CMEs.

EUV solar imagers are currently operating onboard the Proba-2, STEREO (*Solar Terrestrial Relations Observatory*) and SDO (*Solar Dynamic Observatory*) missions while two more imagers are under construction for future space experiments. A project for automatic recognition of eruptive dimmings for post-processed SDO data was recently initiated by NASA (Martens *et al.*, 2011) using detection principles similar to that of NEMO (Attrill and Wills-Davey, 2010). Similar principles have been also used for automated flare detection based on EUV images by de Patoul *et al.* (2008) while Slemzin, Kuzin, and Bogachev (2005) demonstrated a principle to detect eruptive dimmings that are widely distributed in the visible EUV solar corona.

The increased cadence and resolution of STEREO EUV data provided observations of EUV waves that were shorter in time and smaller in size and could not be detected by the NEMO algorithm. As a consequence, it became necessary to develop further the detection efficiency of NEMO. In this work, recent developments and results of the updated NEMO code are presented. These updates have resulted in an increase of the recognition efficiency of the events linked to CMEs. In particular, these updates provide:

- i) the true (de-projected) surface area of the dimming region calculated from the EIT images that are projections onto the solar surface;
- ii) an optimized clustering technique for the extraction of dimming regions;

iii) new criteria for the identification of eruptive dimmings based on their complex characteristics (area and intensity).

The basic scheme of the NEMO algorithm is described in the next section and the most recent developments in Section 3. Some examples are presented in Section 4 and Section 5 offers a conclusive summary.

2. The NEMO Algorithm

The NEMO algorithm consists of two main parts that are briefly presented below.

Event Detection: The first part refers to the detection of events on the EUV solar disk and is based on the behavior of higher-order moments of the image sequences during such events. All discovered types of CME precursor in EUV, such as various EUV waves and sudden loop opening events, are triggered by solar flares or sudden disappearance of filaments (disparition brusques) and they always contain eruptive dimmings. Consequently, all these events strongly affect the probability distribution functions (PDF) of pixels. The techniques that allow the extraction of the eruptive features from the EUV solar disk under complex solar conditions are based on the analysis of skewness and kurtosis. Skewness is a measure of the asymmetry of the PDF. If the left tail of the PDF is more pronounced than the right, then the distribution has negative skewness; when the reverse is true, it has positive skewness. Kurtosis measures the excess probability (flatness) in the tails, where excess is defined in relation to a Gaussian distribution. Large values of higher-order moments indicate the existence of intermittent/bursting events which are characterized by strongly non-Gaussian PDFs (Sandberg *et al.*, 2009). The sudden appearance of coherent and intensive structures on the Sun is reflected by bursts of skewness and kurtosis of the pixel distribution. The appearance of these bursts is a reliable indicator of the occurrence of a flare or an EUV wave.

EUV waves are barely seen in the images due to their low intensity in contrast to the simultaneously appearing solar flare. Thus, base difference (BD) images are constructed by subtracting from images a reference image of the day and taking into account the solar differential rotation. The first step in NEMO is the detection of bursts in higher-order moments in the BD images. This detection principle is very robust and can be applied successfully to data from any EUV telescope, especially in the case of large-scale events. An event is detected when the moments grow in a few consecutive images.

As a “*worst case*” example, let us consider the four faint CMEs observed on 1 April 1997 by the LASCO coronagraph. Their recognition is not distinctive by visual inspection of the SOHO/EIT 195 Å images of the full Sun (Figure 1a). However, the asymmetry and flatness of the pixel distributions on the BD images are excellent indicators of their occurrence (Figure 1b). Remarkably, these CME signatures are observed up until a couple of hours prior to the associated coronagraph observations.

Recognition of Eruptive Dimmings: Once the occurrence of an event has been identified, the second main part of the NEMO code serves to recognize if the *eruptive dimming* is present on the BD image of the solar disk. Eruptive dimmings appears as a region of dark intensity in the EUV wavelengths. However, there are many regions of dark intensity that are continuously present on the EUV Sun. The eruptive dimmings differ from them as they appear rapidly and have the tendency to expand much more quickly.

The algorithm of recognizing eruptive dimmings includes the following consecutive steps:

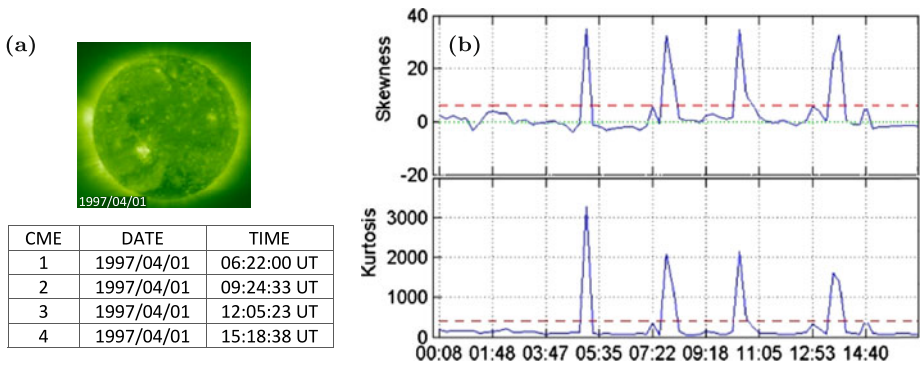


Figure 1 High cadence synoptic observations of the solar disk with SOHO/EIT at a wavelength of 195 Å. The burst in higher-order moments of intensity distributions corresponds to CME initiation observed on this day. (a) 195 Å EIT image at 06:22 UT. (b) Time series of skewness and kurtosis constructed for every image on 1 April 1997. The dashed lines correspond to the value of the standard deviation of the skewness (upper panel) and the kurtosis (lower panel) for the time series of the previous 30 days, and it can be used as a threshold for the identification of detected events. The listed times correspond to the first appearance of CME in the white light LASCO image.

1. *Construction of base differences* with solar differential rotation compensated. The first image before the solar event is subtracted from all the subsequent images.
2. *Extraction of regions with decreased intensity* from the difference images: The regions are extracted by selecting 5% of the darkest pixels in the BD images. The resulting images contain large-scale distinctive regions of reduced intensity. However, small-scale scattered regions of reduced intensity attributed to the presence of noise effects may still remain.
3. *Application of median filtering* for the reduction of small-scale noise: Using this standard procedure, the small-scale scattered noisy points are reduced.
4. *Clustering of decreased intensity regions*: Dimmings are large-scale connected regions of reduced intensity compared to the scattered points attributed to noise. For the extraction of the dimming region, agglomerative filtering is applied; for each reference pixel of reduced intensity with coordinates x_i, y_i the agglomerative weight $W(x_i, y_i)$ is computed. This weight is equal to the number of pixels with reduced intensity in the limited square vicinity around the reference pixel and permits the separation between the small scattered and the large-scale regions of negative intensity.
5. *Dimming Extraction*. For the extraction of a large dimming area from the background of decreased intensity regions, we set the maximum weight $M = \max_i \{W(x_i, y_i)\}$ and we select those pixels with weight that exceeds $q * M$, where $q \in [0; 1]$ is the coefficient of agglomeration. Throughout the present studies, we have retained the value of the coefficient equal to $q = 0.5$.

Figure 2 shows the five steps of dimming extraction as described above using SOHO/EIT 195 Å images taken on 12 May 1997 at 05:07 UT (top panel) and 7 April 1997 at 14:22 UT (bottom panel). If the resulting filtered image contains more than one dimming area, the largest one is selected for subsequent analysis. The growth of the dimming area in a few images determines whether a dimming is eruptive or not.

The algorithm of extracting eruptive dimmings can be summarized as follows:

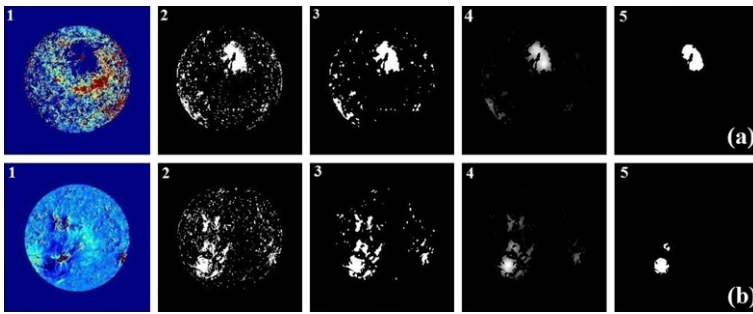


Figure 2 Five steps of dimming extraction from a SOHO/EIT 195 Å image. (a) 12 May 1997 at 05:07 UT and (b) 7 April 1997 at 14:22 UT.

- A positive answer on the first part corresponds to the detection of a burst in the moments of intensity distribution over pixels and provides an alert of the occurrence of an EUV wave.
- A positive answer on the second part corresponds to a growth of the dimming area and provides an alert about EUV wave occurrence and the prompt appearance of a CME in the heliosphere.

The identification of dimming regions may provide early detection of CMEs.

3. Modification of the Algorithm for Dimming Extraction

The dimming extraction by NEMO as presented above was based on the estimation of the dimming area in terms of pixel numbers. However, areas of equal true size at the image center and at the solar limb may differ up to five times in terms of pixel numbers due to projection effects. As a consequence, this may lead to unjustified comparisons of regions with decreased intensity and finally to the loss of events occurring near the limb in favor of smaller dimmings located at the center of the disk.

The clustering technique (agglomerative filtering) of decreased intensity regions uses the square vicinity around a central pixel and the information is taken from an area that is actually the projection of a square to a hemisphere. This can significantly distort the dimming area to be extracted due to the asymmetry of the vicinity relative to its center.

The extraction of an eruptive dimming is carried out by comparing the size of the decreased intensity regions and not the intensity itself. However, the intensity of the dimming is also a significant characteristic (Bewsher, Harrison, and Brown, 2008). The energy released during the dimming formation is almost equal to the energy of the CME (Fillipov, 2007). A joint consideration of dimming areas and intensities can provide an estimation on the power of the CME (Zhukov and Auchère, 2004) and can therefore increase the reliability of the extraction of eruptive dimmings.

In order to improve the detection efficiency of NEMO, the following updates have been applied:

- *Estimation of dimming areas in km².* The dimming area is now computed in terms of square kilometers instead of EIT (or EUVI) pixels by taking into account that an EUV image is a projection of a three-dimensional object onto the solar spherical surface. Using the surface integral and the mean value theorem, we can calculate the surface area of the

i th pixel in km^2 . The total dimming area $S[\text{km}^2]$ is simply determined by the sum of the pixel areas. The total dimming area $S[\text{km}^2]$ is simply determined by the sum of the pixels surface $S = \sum_D S_i$ that form the dimming area D .

- *Clustering in circle vicinity.* The clustering procedure is significantly improved since the agglomerative filtering is carried out on a spherical surface of a circular vicinity. We have found that this approach improves the accuracy of the extraction of dimming structure.
- *Complex characteristic for dimming extraction.* In order to increase the confidence of the dimming extraction, the NEMO algorithm uses a new characteristic variable that is defined by the sum of the products of dimming pixel intensity I_i and pixel area S_i over the dimming region D :

$$\mathcal{I} = \sum_D \mathcal{I}_i = \sum_D I_i \cdot S_i.$$

This variable is essentially given by the surface integral of the intensity over the dimming region and can be considered as the total intensity of the dimming region on the Sun.

It can be used for the construction of a more qualitative picture of the evolution of a dimming in time and provides a rough measure of the CME power connected with the formation of the dimmings considered.

In order to validate the updated dimming extraction algorithm we performed a limited series of comparative studies with the widely used growing-region technique (Gao, Wang, and Zhou, 2002; Podladchikova and Berghmans, 2005; see also Attrill *et al.* (2006) and Robbrecht and Berghmans (2005) for a review).

The growing region technique is considered to be an accurate approach but it is unsuitable for fast automated extraction due to its slow performance. Remarkably, the regions extracted using the updated algorithm and the growing region technique were similar.

4. Comparison Between the Tested and Basic Algorithms

A comparative analysis between the updated and the basic NEMO algorithms has been carried out based on a number of SOHO and STEREO EUV observations of the solar corona. Furthermore, results of the proposed improved technique have been compared with CME detection results of the CACTUS software based on coronagraph data.

It was clearly shown that the new algorithm provides a more accurate estimation of the shape and size of eruptive dimmings for all the considered cases. The modified algorithm is more sensitive to small-scale events and provides much earlier detection, while the basic algorithm could completely overlook small-scale events. Remarkably, the results are effectively improved for events observed near the solar limb. Three characteristic examples are presented below.

Improved Processing of Dimmings An eruptive event was observed near the solar limb by the SOHO/EIT imaging telescope in the 195 \AA wavelength on 7 April 1997 at 14:22 UT. This event was automatically detected in both basic and modified algorithms. Figure 3 depicts the structures extracted from the difference images using the basic (Figure 3a) and the modified (Figure 3b) algorithms. As shown, the modified algorithm demonstrates a considerably more precise definition of the dimming shape. The area of the dimming is given in km^2 instead of pixels, while a number of additional parameters are also provided.

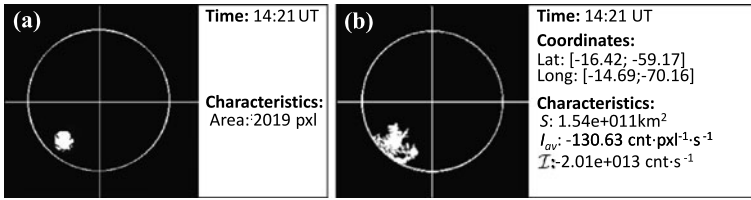


Figure 3 More precise extraction of the dimming of the 7 April 1997 SOHO/EIT event by the modified algorithm with respect to the dimming extracted by the basic NEMO method (a). More dimming characteristics are provided by the modified extraction algorithm (b).

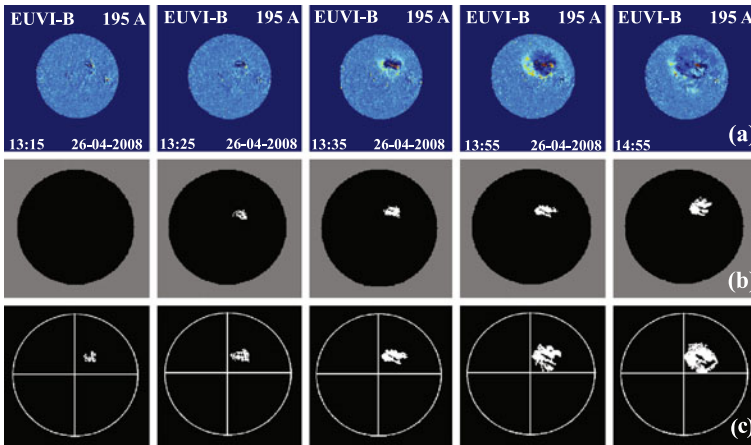


Figure 4 The 26 April 2008 STEREO/EUVI event, detected with delay by the basic algorithm. (a) Differences images, (b) dimmings extracted by the basic algorithm, and (c) dimmings extracted by the modified algorithm with characteristics indicated in Table 1.

Improved Detection Efficiency The STEREO-B/EUVI observations of the solar disk eruptive event that occurred on 26 April 2008 from 13:15 UT to 13:55 UT are shown in Figure 4. The top panel depicts the BD images of the event created by subtracting a reference image before the event onset from the subsequent images. The middle and bottom panels show the dimmings extracted using the basic and the modified algorithms respectively. As shown, the modified version of the algorithm detects the dimming from the early stages of the event development (at 13:15 UT) in contrast to the basic algorithm, which provides a detection alert with a relative delay of 10 min. The parameters of the event are shown in Table 1 as extracted by using the new algorithm. The basic algorithm cannot provide the shape and the rest of the characteristic parameters of the eruptive dimming with such accuracy.

Detection of Small-Scale Events The improved spatial and temporal resolution of the EUVI telescope onboard the STEREO spacecraft has permitted the observation of smaller eruptive images with respect to those observed before the upgrade of the instrument (Innes *et al.*, 2009; Podladchikova *et al.*, 2010; Innes, McIntosh, and Pietarila, 2010). A relatively small-scale event was captured by the STEREO-B/EUVI telescope on 23 April 2003 between 06:05 UT and 07:35 UT. The basic algorithm could not issue an alert of eruptive dimming in this case, yet the updated algorithms did successfully. The BD images and the

Table 1 Characteristics of 26 April 2008 STERO/EUVI event (eruptive dimming) extracted by the modified NEMO algorithm.

Time [UT]	Latitudes [degree]	Longitudes [degree]	Area [km ²]	Average intensity [count pixel ⁻¹ s ⁻¹]	Total intensity [count s ⁻¹]
13:15	9.09; 20.46	11.86; 22.25	8.86e+009	-1.48e+002	-1.31e+012
13:25	9.23; 20.48	3.08; 21.71	1.09e+010	-2.70e+002	-2.95e+012
13:35	10.26; 23.41	3.07; 21.15	3.69e+010	-3.78e+002	-6.40e+012
13:55	1.63; 28.55	0.78; 27.76	5.14e+010	-5.37e+002	-2.76e+013
14:05	0.89; 27.76	0.15; 30.68	6.75e+010	-4.82e+002	-3.25e+013

Table 2 Characteristics of the 23 April 2008 small-scale EUVI/STEREO event, detectable only by using the modified algorithm.

Time [UT]	Latitudes [degree]	Longitudes [degree]	Area [km ²]	Average intensity [count pixel ⁻¹ s ⁻¹]	Total intensity [count s ⁻¹]
06:05	9.33; 21.40	-31.39; -41.48	9.38e+009	-1.79e+002	-1.68e+012
06:25	9.31; 23.87	-29.38; -41.49	1.22e+010	-3.72e+002	-4.52e+012
06:45	2.32; 23.91	-28.35; -44.57	1.67e+010	-4.41e+002	-7.36e+012
07:15	1.55; 23.93	-26.36; -45.95	2.06e+010	-5.46e+002	-1.13e+013
07:35	-3.87; 23.95	-26.20; -48.03	2.08e+010	-5.79e+002	-1.20e+013

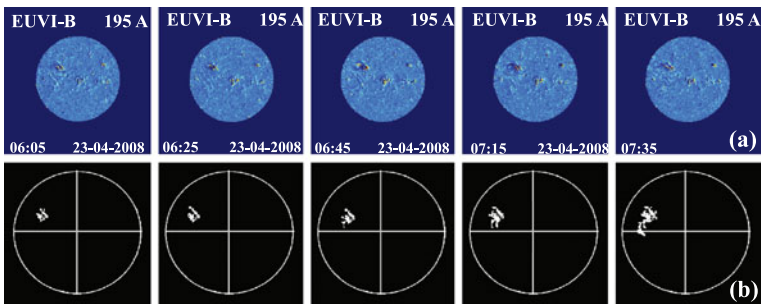


Figure 5 Small-scale dimming of a STEREO/SECCHI event, detectable only by using the modified algorithm. (a) 06:05 UT–06:35 UT difference images of the 23 April 2008 STEREO-B/EUVI event. (b) Extracted dimmings with the characteristics given in Table 2.

extracted dimming by the modified algorithm are shown in the top and bottom panels of Figure 5, respectively, while characteristics of the extracted event are given in Table 2.

From all the examples presented above it is evident that consideration of both the area and intensity of the dimming region, in combination with circle vicinity clustering in spherical coordinates, significantly increases the detection efficiency and the information provided by the extracted dimmings.

In order to show the importance of the new improvements in the NEMO code, we present here the results of a comparative study with the basic NEMO algorithm for the period of

20 March 2008 to 26 April 2008 that includes the so-called Whole Heliospheric Interval (WHI). For this period, the updated algorithm provides the detection of 55 eruptive events using STEREO-A/EUVI 195 Å data and 60 eruptive events using STEREO-B/EUVI 195 Å data. Five out of 55 and four out of 60 detected events from STEREO-A and -B were false positive, respectively. For the same time period, the basic NEMO algorithm could provide the detection of 37 events from STEREO-A/EUVI 195 Å data and 36 eruptive events from STEREO-B/EUVI 195 Å data. In particular, four out of 37 and three out of 36 detected events from STEREO-A and -B were false positive, respectively. Thus, the number of true positive events detected by the updated algorithm during the WHI period increased by 30%, while the number of false positive events practically did not change. Noticeably, the CACTUS software provided the detection of 31 and 24 CMEs, respectively, using the coronagraph data from STEREO-A and STEREO-B, respectively.

The updated version of NEMO will include the schemes presented and will introduce the following parameter values in the NEMO catalogs of eruptive events:

- Coordinates of the dimming (latitudes and longitudes of the dimming borders)
- Intensity of the dimming I
- The surface integral of the intensity over the dimming region \mathcal{I}
- Area of the dimming region in km^2

As a consequence, the NEMO catalogs will provide additional information about the signatures of detected CMEs.

5. Conclusions

We have developed novel algorithms for the NEMO detection tool for flares and CMEs, for post-processes of SOHO/EIT and STEREO/SECCHI EUV solar disk images. The NEMO version consists of two main parts, namely Event Detection and Eruptive Dimming Recognition. Event detection is based on the detection of bursts of higher-order moments of images, while the eruptive dimming extraction is based on the application of filtering techniques applied to image sequences. In this work, we have presented a series of updates in the eruptive dimming extraction algorithms that allow us to significantly increase the detection efficiency of eruptive dimmings linked to CMEs.

The area of the dimming region is now computed directly in terms of physical variables (square kilometers) by taking into account that EIT images correspond to the projections of three-dimensional structures onto the solar surface. The clustering of dark regions is achieved through circle vicinity clustering on the latitude and longitude. Furthermore, novel methods for the eruptive dimming extraction – based on the surface integral of the intensity over the dimmings – increase the detection efficiency and accuracy of the associated extracted parameters. Using a series of examples, we have shown that the modified version of the NEMO tool presents significantly higher temporal and spatial efficiency regarding the automatic detection of CME signatures. In particular, small eruptive events located near the solar limb can be detected now while major events can be detected earlier than before. As a result the detection efficiency of the updated scheme increased by 30% according to the comparative studies performed for STEREO/EUVI 195 Å data for the period of WHI. The NEMO tool will incorporate the new optimized algorithms and it is expected to provide early warnings for CMEs and to automatically construct new catalogs with enhanced and more accurate information.

Acknowledgements A.V. and P.L. acknowledge the ASBL–VZW research grant for MSc studies on “Dynamics of the Solar System” at the Royal Observatory of Belgium. The authors would like to thank the anonymous referee for suggestions and insight in improving this article.

References

- Atrill, G., Nakwacki, M.S., Harra, L.K., van Driel-Gesztelyi, L., Mandrini, C.H., Dasso, S., Wang, J.: 2006, Using the evolution of coronal dimming regions to probe the global magnetic field topology. *Solar Phys.* **238**, 117–139.
- Atrill, G.D.R., Wills-Davey, M.J.: 2010, Automatic detection and extraction of coronal dimmings from SDO/AIA data. *Solar Phys.* **262**, 461–480.
- Bewsher, D., Harrison, R.A., Brown, D.S.: 2008, The relationship between EUV dimming and coronal mass ejections. I. Statistical study and probability model. *Astron. Astrophys.* **478**, 897–906.
- Biesecker, D.A., Myers, D.C., Thompson, B.J., Hammer, D.M., Vourlidas, A.: 2002, Solar phenomena associated with “EUV waves”. *Astrophys. J.* **569**, 1009–1015.
- de Patoul, J., Berghmans, D., Nicula, B., Podladchikova, O.: 2008, Solar flare detector for EUV images. In: Irland, J., Young, C., Delouille, V. (eds.) *Solar Image Processing Workshop IV*, 10.
- Delaboudinière, J.-P., Artzner, G.E., Brunaud, J., Gabriel, A.H., Hochedez, J.F., Millier, F., et al.: 1995, EIT: Extreme-ultraviolet Imaging Telescope for the SOHO mission. *Solar Phys.* **162**, 291–312.
- Fillipov, B.P.: 2007, *Physics of the Solar Corona: An Introduction, Fundamental and Applied Physics*, Fizmatlit, Moscow, 1–335.
- Gao, J., Wang, H., Zhou, M.: 2002, Development of an automatic filament disappearance detection system. *Solar Phys.* **205**, 93–103.
- Gopalswamy, N.: 2004, A global picture of CMEs in the inner heliosphere. In: Poletto, G., Suess, S. T. (eds.) *The Sun and the Heliosphere as an Integrated System*, Kluwer Academic, Dordrecht, 201–217.
- Gosling, J.T., Thomsen, M.F., Bame, S.J., Russell, C.T.: 1990, Cold ion beams in the low latitude boundary layer during accelerated flow events. *Geophys. Res. Lett.* **17**, 2245–2248.
- Harra, L.K., Sterling, A.C.: 2001, Material outflows from coronal intensity “dimming regions” during coronal mass ejection onset. *Astrophys. J. Lett.* **561**, L215–L218.
- Innes, D.E., McIntosh, S.W., Pietarila, A.: 2010, STEREO quadrature observations of coronal dimming at the onset of mini-CMEs. *Astron. Astrophys.* **517**, L7.
- Innes, D.E., Genetelli, A., Attie, R., Potts, H.E.: 2009, Quiet Sun mini-coronal mass ejections activated by supergranular flows. *Astron. Astrophys.* **495**, 319–323.
- Kahler, S.W.: 1992, Solar flares and coronal mass ejections. *Annu. Rev. Astron. Astrophys.* **30**, 113–141.
- Martens, P.C.H., Atrill, G.D.R., Davey, A.R., Engell, A., Farid, S., Grigis, P.C., et al.: 2011, Computer vision for the Solar Dynamics Observatory (SDO). *Solar Phys.* doi:[10.1007/s11207-010-9697-y](https://doi.org/10.1007/s11207-010-9697-y).
- Plunkett, S.P., Thompson, B.J., Howard, R.A., Michels, D.J., St. Cyr, O.C., Tappin, S.J., Schwenn, R., Lamy, P.L.: 1998, LASCO observations of an Earth-directed coronal mass ejection on May 12, 1997. *Geophys. Res. Lett.* **25**, 2477–2480.
- Podladchikova, O., Berghmans, D.: 2005, Automated detection of EIT waves and dimmings, *Solar Phys.* **228**, 265–284.
- Podladchikova, O., Vourlidas, A., Van der Linden, R.A.M., Wülser, J., Patsourakos, S.: 2010, Extreme ultraviolet observations and analysis of micro-eruptions and their associated coronal waves. *Astrophys. J.* **709**, 369–376.
- Richardson, I.G., Cliver, E.W., Cane, H.V.: 2001, Sources of geomagnetic storms for solar minimum and maximum conditions during 1972–2000. *Geophys. Res. Lett.* **28**, 2569–2572.
- Robbrecht, E., Berghmans, D.: 2004, Automated recognition of coronal mass ejections (CMEs) in near-real-time data. *Astron. Astrophys.* **425**, 1097–1106.
- Robbrecht, E., Berghmans, D.: 2005, Entering the era of automated CME recognition: A review of existing tools. *Solar Phys.* **228**, 239–251.
- Sandberg, I., Benkadda, S., Garbet, X., Ropokis, G., Hizanidis, K., del-Castillo-Negrete, D.: 2009, Universal probability distribution function for bursty transport in plasma turbulence. *Phys. Rev. Lett.* **103**, 165001.
- Slemzin, V., Kuzin, S., Bogachev, S.: 2005, Temporal and spatial dynamics of CME-related solar structures from EUV observations with the Coronas-F and SOHO/EIT telescopes. In: Danesy, D., Poedts, S., De Groof, A., Andries, J. (eds.) *The Dynamic Sun: Challenges for Theory and Observations, ESA SP-600*, 166.1 (on CDROM).
- Thompson, B.J., Myers, D.C.: 2009, A catalog of coronal “EUV wave” transients. *Astrophys. J. Suppl.* **183**, 225–243.

- Thompson, B.J., Plunkett, S.P., Gurman, J.B., Newmark, J.S., St. Cyr, O.C., Michels, D.J.: 1998, SOHO/EIT observations of an Earth-directed coronal mass ejection on May 12, 1997. *Geophys. Res. Lett.* **25**, 2465–2468.
- Zhukov, A.N.: 2004, Initiation of CMEs: EIT waves and EUV dimmings. In: Sakurai, T., Sekii, T. (eds.) *The Solar-B Mission and the Forefront of Solar Physics*, *ASP Conf. Ser.* **325**, 381–388.
- Zhukov, A.N., Auchère, F.: 2004, On the nature of EIT waves, EUV dimmings and their link to CMEs. *Astron. Astrophys.* **427**, 705–716.